Quantitative Identification of Temporal-Spatial Variations of Urban Heat Island (UHI) Effects in Changchun, China

Ziqi Chen and Yanhong Zhang

***Abstract*—With the fast urbanization, urban heat island (UHI) effect is becoming more and more pronounced. Identify and evaluate the temporal-spatial variations and the driving factors that are in urgent need to alleviate a series of problems caused by heat island. Changchun of Jilin province is located in northeast China, using multiperiod satellites images and other ancillary data to invert the surface temperature and acquire the surface land cover classification, then it analyzed the temporal-spatial variation of UHI effect and relation between urban developments. The temporal variations of UHI effects based on air temperature (AT) showed: the UHI was strong at night and weak in daytime; the UHI was strong in autumn and winter and weak in spring and summer; the UHI effect increased rapidly before 2015 and decreased after 2015. The spatial variations of UHI based on land surface temperature (LST) effected: The area of higher temperature zone increased, while the area of other areas declined. The strength order of the UHI effect for different land surface covering types was: building land＞ grassland＞ woodland＞water area. This meant how to layout urban land use types were important, reasonable urban land planning was necessary for urban sustainable development. This study provided an important basis for counteracting the UHI effect and promoting the construction of an eco-city.**

***Index Terms*—Changchun, spatial-temporal variation, temperature inversion, urban heat island (UHI) effect.**

I. Introduction

AFTER the first time, the concept of "urban heat island(UHI)" was put forward by Howard [1], [2]. The UHI effect has always been a hot research area with both theoretical and practical significance in the late 20th century [3], [4], with the global warming and rapid urbanization. Moreover, climate change caused by urbanization has affected the urban thermal environment more directly than global climate change [5], [6]. This meant UHI caused by urbanization was the main body of urban climate change and should be our key concern. Actually, quite a number of research works focused on UHI intensity and the spatial-temporal differences. UHI intensity was a crucial indicator of the size of the UHI effect in urbanized areas. A conventional method to evaluate UHI was determined by comparing the average and maximum air temperature (AT) between an urban (Tu) and rural area (Tr). The limitation of UHI intensity calculation was that it was not possible to obtain accurate data for the desired area due to temporal and spatial constraints [3]. For the spatial and temporal variation, the UHI has always been complicated due to the heterogeneous geographical space. Along with the short-, medium-, and long-term, the UHI showed significant diurnal, seasonal, and interannual variations. For example, the study showed that the seasonal characteristics of Beijing UHI were obvious, and the maximum heat island intensity appeared in summer. While the spatial distribution was characterized in mosaic distribution by scattered hotspot and patches of heat island; the cold island appeared in winter, and its spatial distribution was consistent with the Summer UHI; the UHI was the smallest in Spring and Autumn [7]. While for the micro-, meso-, and macro-scales, UHI showed significant spatial variability, which was clearly related to the nature and cover type of the substratum. Some studies pointed out that the future research works should focus on the coastal and complex topography that may be the main causes that induced the UHI effects, in order to explore various factors and the influence of superposition and accumulation on UHI effect [8]–[19]. Some scholars also considered the relationship between different climate regions and UHI [20]. In high latitude regions, the atmospheric pollution would be aggravated in winter due to the existence of the heat island effect, and a suspended inversion layer would be formed in the lower atmosphere of the high-temperature region of the heat island, which could directly hinder the diffusion of pollutants in the atmosphere [21]. Under normal circumstances, urban air pollution such as smoke and dust would be more than the air in the suburbs. Especially when the sun was rising, it would be more likely to produce harmful photochemical pollutants. With the urban area expansion, the previously polluted industrial areas might be gradually covered by the new heat island area, and the heat island circulation could bring pollutants from the old industrial area to the urban area that would increase the atmospheric pollution scope in urban areas [22]. It could be seen that the UHI effect might cause a greater impact on the sustainable developments [23]. Although many studies on the UHI effects have been conducted in many big cities all around the world [24]. However, due to the complexity

Manuscript received December 24, 2021; revised February 9, 2022 and March 18, 2022; accepted April 12, 2022. Date of publication April 19, 2022; date of current version May 3, 2022. This work was supported in part by the National Key R&D Program of China under Grant 2016YFC0500204. *(Corresponding author: Yanhong Zhang.)*

The authors are with the College of Geo-exploration Science & Technology, Jilin University, Changchun 130026, China (e-mail: chenzq0227@163.com; giswork@163.com).

Digital Object Identifier 10.1109/JSTARS.2022.3167831

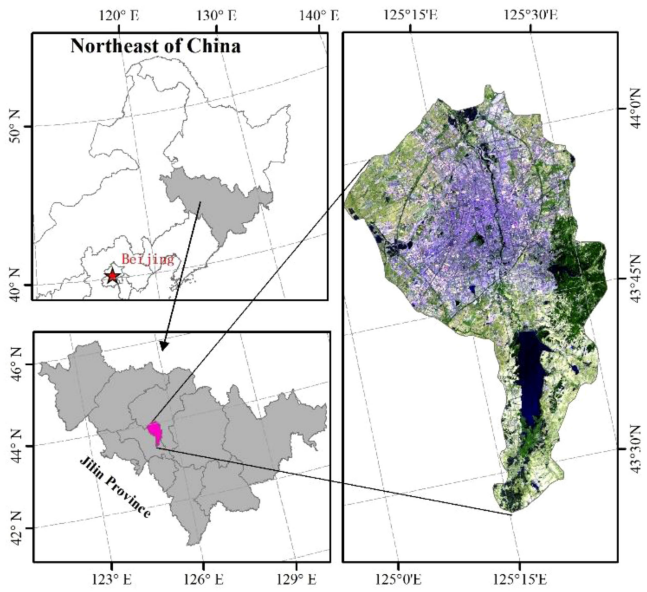

Fig. 1. Location map of study area.

and variability of UHI, even if the same city, because of different parameters, the UHI showed great changes [25], for example, the heat island intensity calculated based on land surface temperature (LST) and AT was very different [26]. Especially for the high-latitude region, the climate showed high latitudes exhibit dramatic changes in weather and climate to further explore the variation of UHI, especially how to use advanced remote sensing technology to identify the temporal-spatial variations of UHI effects was very important for the future urban land planning and urban development. This study took Changchun and explored the spatial distribution characteristics of the UHI effect from 2000 to 2020. The main objectives were to

1) analyze the time variation characteristics of the UHI effect in day, season, and year based on AT;
2) identify the spatial change trend of the UHI effect through temperature classification and gradient analysis based on LST; and
3) analyze the degree of the UHI effect caused by different land use types.

II. Study Area and Data

A. Study Area

Changchun city of Jilin province is located in northeast China, which is in 43°05'–45°15'N, 124°18'–127°05'E (see Fig. 1). Because of the typical north temperate continental monsoon, Changchun is in the transition zone from humid to subarid regions. The temperature increases from the east region to the west and the precipitation decreases from the east region to the west. Changchun has four distinct climatic characteristics: dry and windy in spring, hot and humid and rainy in summer, cool in autumn, and cold and long in winter. It is an ideal experience area to explore the UHI effect because its district needs heating in cold winter and the old industrial area is polluted by heat island effects.

TABLE I
Remote Sensing Data

Time	Date	SPACECRAFT_ID
2000	2000/09/26	LANDSAT_5
2007	2007/08/29	LANDSAT_5
2014	2014/09/17	LANDSAT_8
2020	2020/08/16	LANDSAT_8

B. Remote Sensing Data and Data Preprocessing

The images used for this article are Landsat images for Changchun city area downloaded from the geospatial data cloud (see Table I). The two scenes image cover the whole area with strip code 118 29 and 118 30. After atmospheric radiometric calibration, geometric correction, and image mosaic including setting the background value, feather value, and uniform light, the complete Changchun Images were obtained.

C. Other Data

The atmosphere transmittance was obtained by looking up the moisture content of the atmosphere on the NASA[1] and the average atmosphere temperature was obtained by looking up the data.

In order to analyze the temporal variation of temperature and verify its consistency with the remote sensing image temperature, we obtained the temperature data of Changchun station for the same period, and further developed the daily, seasonal, and annual temperature information.

III. Math and Process

A. LST Inversion

To explain the proposed temporal-spatial analysis method of the UHI effect, a flowchart was shown in Fig. 2, which provided an overview of detailed steps to inversion the LST using the mono window algorithm from a series of Landsat images.

Through the radiative transfer equation, Landsat thermal infrared data can establish a direct contact with LST [27], the mono window algorithm was developed by Qin [28]. The radiation temperature was calculated by the radiation intensity, and the surface emissivity was calculated by NDVI and vegetation coverage [29]. T_s can be calculated as follows:

$$T = \frac{\{a\,(1-C-D)+[b\,(1-C-D)+C+D]\,T_{\text{sensor}}-DT_a\}}{C} \tag{1}$$

where T is the LST, T_{sensor} is the radiant brightness of the thermal infrared band, T_a is the estimated average atmospheric temperature, it is calculated by the relationship between the temperature (T_0) close to the ground (about 2 m from the ground) [30]. a and b are the fitting coefficients, when the surface temperature

[1][Online]. Available: http://atmcorr.gsfc.NASA.gov/

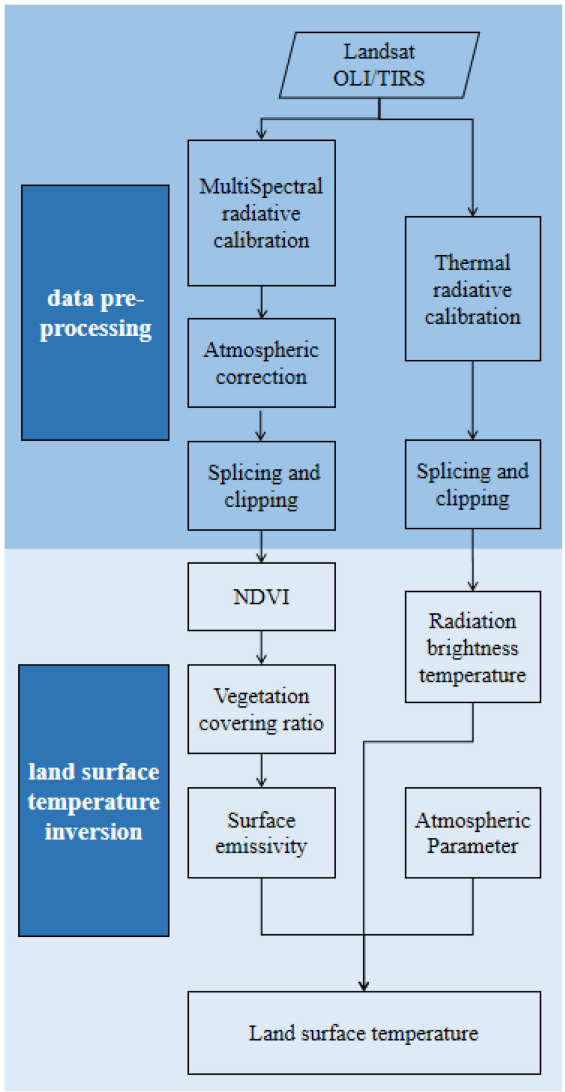

Fig. 2. Flowchart.

is between 0–70 °C, a = -67.355351, b = 0.458606. C, D, and T_{sensor} can be calculated as follows:

$$C = \varepsilon\tau \tag{2}$$

$$D = (1-\tau)\,[1+(1-\varepsilon)\,\tau] \tag{3}$$

$$T_{\text{sensor}} = \frac{K_2}{\ln\left(1+\frac{K_1}{L_\lambda}\right)} \tag{4}$$

where C and D are the intermediate variables based on the surface emissivity and atmospheric transmittance, K_1 and K_2 are preset constants before the satellite launch, L_λ is the spectral radiation value after image thermal infrared band preprocessing. τ is the transmittance of the atmosphere on that day, it is the basic parameter of surface temperature inversion, due to the influence of many factors, it is difficult to calculate its accurate value and can be estimated by the atmospheric transmittance model [31]

$$\varepsilon = \begin{cases} \varepsilon_{\text{water}} = 0.995 \\ \varepsilon_{\text{surface}} = 0.9625 + 0.0614{*}\mathrm{F}_v - 0.0461{*}\mathrm{F}_v{*}\mathrm{F}_v \\ \varepsilon_{\text{building}} = 0.9589 + 0.086{*}\mathrm{F}_v - 0.0671{*}\mathrm{F}_v{*}\mathrm{F}_v \end{cases} \tag{5}$$

TABLE II
TEMPERATURE GRADING CHART

Temperature class	Range
Highest temperature zone	T>μ+σ
Higher temperature zone	μ+0.5σ<T<μ+σ
Medium temperature zone	μ-0.5σ<T<μ+0.5σ
Lower temperature zone	μ-σ<T<μ-0.5σ
Lowest temperature zone	T<μ-σ

where ε represents the specific emissivity of the surface, refers to the ratio of the radiation emitted by the surface to the radiation emitted by the blackbody at the same temperature [32], for most surface materials (water, vegetation, rock, and soil), the specific emissivity value is usually between 0.93 and 0.99 [33]

$$F_v = \frac{\text{NDVI} - \text{NDVI}_{\text{min}}}{\text{NDVI}_{\text{max}} - \text{NDVI}_{\text{min}}} \tag{6}$$

where F_{v} is the vegetation covering ratio, refers to the percentage of the vertical projected area of vegetation (including leaves, stems, and branches) on the ground in the total area of the statistical area [34]

$$\text{NDVI} = \frac{NIR - R}{NIR + R} \tag{7}$$

where NDVI is the normalized difference vegetation index, NIR and R are the reflectance values at near-infrared band and red band [35].

B. LST Classification

This article selected the mean-standard deviation temperature classification method, which used the combination of the mean (μ) and standard deviation (σ) of the surface temperature to divide the surface thermal field, and also made the UHI form an effective definition. Among them, the standard deviation reflected the deviation degree of the current temperature compared with the average temperature, and the combination of the two can reflect the temperature changes of different ground objects. The specific division criteria were shown in Table II.

C. Rural-Urban Gradient Analysis

In this study, the administrative point of Changchun was selected as the central point and established gradient analysis through concentric multirings of equal width with an interval of 2 km in the urban center (see Fig. 3). A total of 16 km multiring buffer zones was used to identify the gradient change characteristics of the urban thermal environment, and further analysis of the surface temperature changes in each 2 km buffer zone.

IV. RESULTS

The UHI intensity was the numerical value of the temperature higher than the suburban area in the central city, which was expressed by the temperature difference of two representative measuring points. In this study, the urban temperature of Changchun was chosen as the central urban temperature,

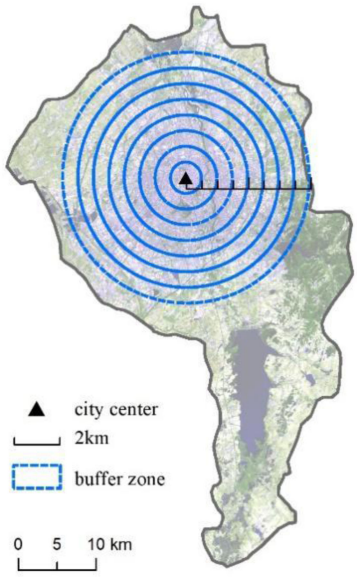

Fig. 3. Buffer distribution map.

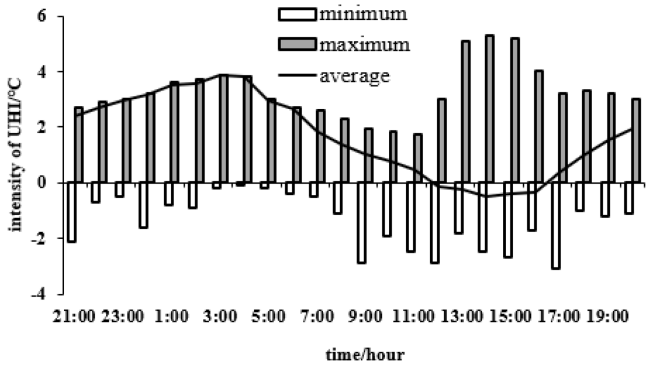

Fig. 4. Daily variation of heat island effect.

and the temperature of Shuangyang district was chosen as the suburban temperature. The Heat Island intensity was defined as: $T = T_{\text{changchun}} - T_{\text{shuangyang}}$.

A. Daily Variation of Heat Island Effect

Based on the data of August 2015 and the definition of the UHI intensity in this article, the temporal difference of the daily UHI intensity as Fig. 4.

The UHI intensity in Changchun was stronger at night and weaker during the daytime. From 12:00 to 16:00, the UHI intensity was negative, the minimum value appeared at 14:00, before and after was −0.5 °C, the UHI intensity was positive at night, and the maximum value appeared at 3:00 in the morning around sunrise, was 3.85 °C, the daily average intensity of UHI was 1.67 °C. According to the solar radiation variation and land surface thermal radiation characteristics, the changes of UHI intensity were mainly caused by the following factors: the surface of the urban area absorbed and stored a large amount of heat during the daytime and radiated it back into the atmosphere at night. At night, the accumulation of pollutants in the urban atmosphere due to the weakening of the convection effect would

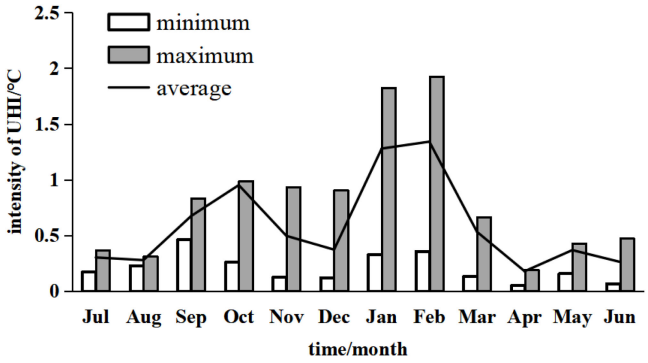

Fig. 5. Seasonal variation curve of heat island effect.

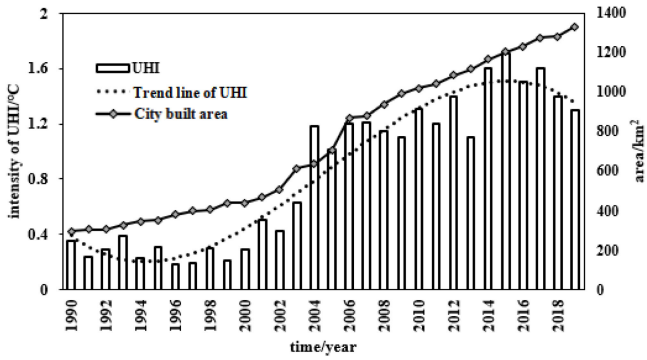

Fig. 6. Annual variation curve of heat island effect.

obviously absorb the long-wave radiation on the ground, and most of them radiated to the ground in the form of inverse radiation, then the radiation inversion was formed and caused the more slowly cooling cities [36]. While the suburbs, fewer buildings and open terrain would make the faster cooling at night. Thus, the UHI was more pronounced at night than during the daytime. After sunrise, the sun could not directly reach the ground in the urban area due to the obstruction of tall buildings. When the altitude angle of the sun was still very low, the ground could directly receive the solar radiation and quickly heat up, causing the urban area to heat up later than the suburb. So, the UHI intensity gradually turned to weaken, the heat island intensity would reach the weakest at noon, even appeared negative value [37].

B. Seasonal Variation of Heat Island Effect

This article presented Changchun meteorological data from 2013 to 2019. The interval data were analyzed statistically and displayed in Fig. 5.

In February and December, the average of the UHI intensity was higher than 1.2 °C. The intensity in September and October was also strong, all above 0.5 °C. The intensity of UHI in other months was weak, among which in June and July was less than 0.3 °C, while the intensity of UHI in April was the lowest. It can be seen that Changchun UHI showed strong in autumn and winter, and weak in spring and summer. According to the analysis of climate seasonal and UHI changes, Changchun was located in the continental area of the northern temperate zone, affected by the monsoon. In spring and summer, the influence of

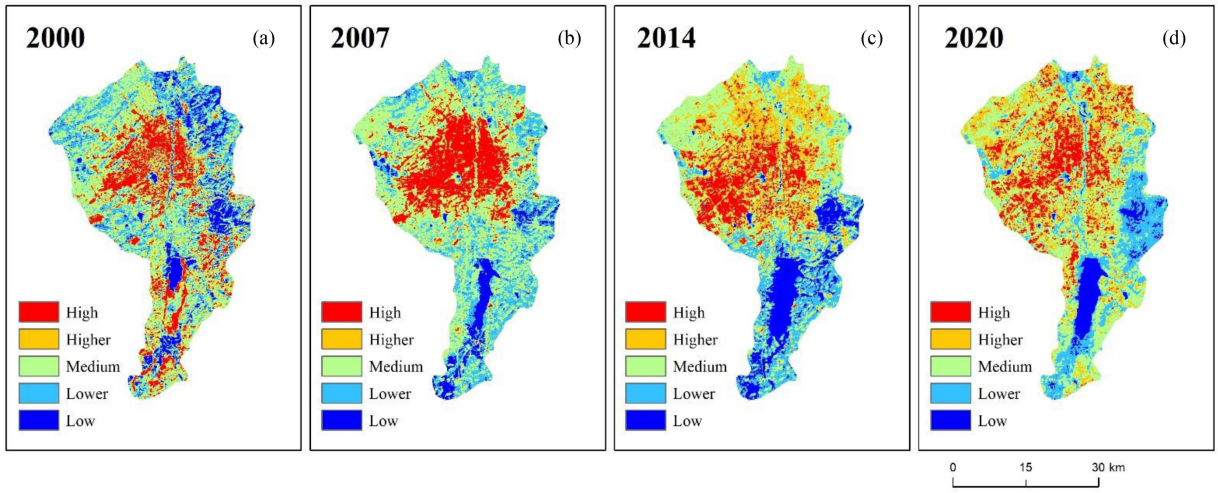

Fig. 7. Temperature grading chart.

the monsoon was serious, the atmospheric state was unstable, the pollutants and heat in the urban atmosphere were easy to diffuse, and the rainfall was more in spring and summer, the evaporation of surface water in the urban area was larger, taking more heat with it. At the same time, the rain water will wash away the air pollutants, while in autumn and winter, under the influence of cold and high pressure, dry and less rain, the atmospheric state was more stable, so the UHI in autumn and winter in Changchun was stronger.

The main reason for the strong UHI in Changchun in winter was that the temperature of Changchun was very lower in winter and a lot of heating were needed. The heat generated by the heating system were most obvious in winter, and the denser population, the bigger city, the heating caused by the phenomenon of rising temperatures in urban areas were more obvious.

C. Annual Change of Heat Island Effect

The annual mean temperature data of Changchun from 1990 to 2019 were obtained from Changchun Meteorological Yearbook displayed in Fig. 6. From the variation trend, the intensity of Changchun heat island fluctuated before 2000, and increased after 2000, showing the characteristics of rapid growth. After 2007, the heat island intensity tended to be stable, with a slight decline trend. The UHI strengthened after 2000 could due to urban expansion during this period, the speed of urbanization accelerated significantly. With the expansion of urban land scale, urban industrial development, the urban water, and green area ratio could decline, which would exacerbate the UHI effect. However, at the end of the period of urban expansion, people's environmental awareness became stronger, the environmental situation has been improved, and the degree of urban greening has increased, which played a certain role in alleviating the UHI effect.

D. Spatial Variation of Heat Island Effect

The acquisition time was different because of the different data types of the images. Compared with the inversion temperature directly, there would be a bigger error. But the relative temperature value was constant. Therefore, this article grad the temperature, in order to compare the temperature of different phases. The distribution area of different temperature zones could be obtained by statistical analysis of the temperature classification map (see Fig. 7). At the same time, the changes of different temperature zones can be obtained in Table III.

The distribution of highest temperature area was more concentrating in 2000. At the same time, there were a few highest temperature areas in the southern part of Changchun. On the one hand, because there were a few uncultivated lands, which would reflect a lot of heat. On the other hand, the total precipitation was relatively small in 2000. The climate was more arid than usual, the water level of Xinlicheng reservoir was lower, the lake bed was exposed a lot, and the bare land would reflect a lot of heat, forming a highest temperature zone. The higher temperature area was located at the edge of the highest temperature area and the boundary of the urban area. The distribution of the medium temperature zone was scattered, which was located in the nonurban area of the city, and most of them were agricultural land. The lower temperature area distributed in Changchun Central part, mostly was the forest land and the grassland. The lowest temperature mainly distributes in Xinlicheng reservoir and the Eastern Mountain area in the west.

In 2007, the peak of urbanization in Changchun, the urban area expanded, resulting in the expansion of the distribution area of highest temperature areas, from 15.35% to 18.34%. The water level of Xinlicheng reservoir was rising and no longer forming a highest temperature zone in the bare lake bed. The higher temperature area was still distributed at the edge of the highest temperature area, which was located in the suburb of the city. The area has reduced from 11.32% to 7.59%. The area of the medium temperature zone has been expanded by 4% and was located on the agricultural land.

The process of urbanization slowed down in 2014, but the degree of urbanization was large and the area of urban areas expanded. Compared with the previous two images, the area of the highest temperature area was reduced by 4.59%. At the same time, the highest temperature zone also appeared in the

TABLE III
STATISTICAL TABLE FOR ANALYSIS OF TEMPERATURE CHANGES

Temperature class	2000(%)	2007(%)	2014(%)	2020(%)	2000-2007(%)	2007-2014(%)	2014-2020(%)
Highest temperature zone	15.35	18.34	13.75	14.51	2.99	-4.59	0.76
Higher temperature zone	11.32	7.59	24.50	23.79	-3.73	16.91	-0.71
Medium temperature zone	40.54	44.54	32.87	37.20	4.00	-11.67	4.33
Lower temperature zone	22.39	23.12	17.09	18.35	0.73	-6.03	1.26
Lowest temperature zone	10.40	6.41	11.79	6.15	-3.99	5.38	-5.64

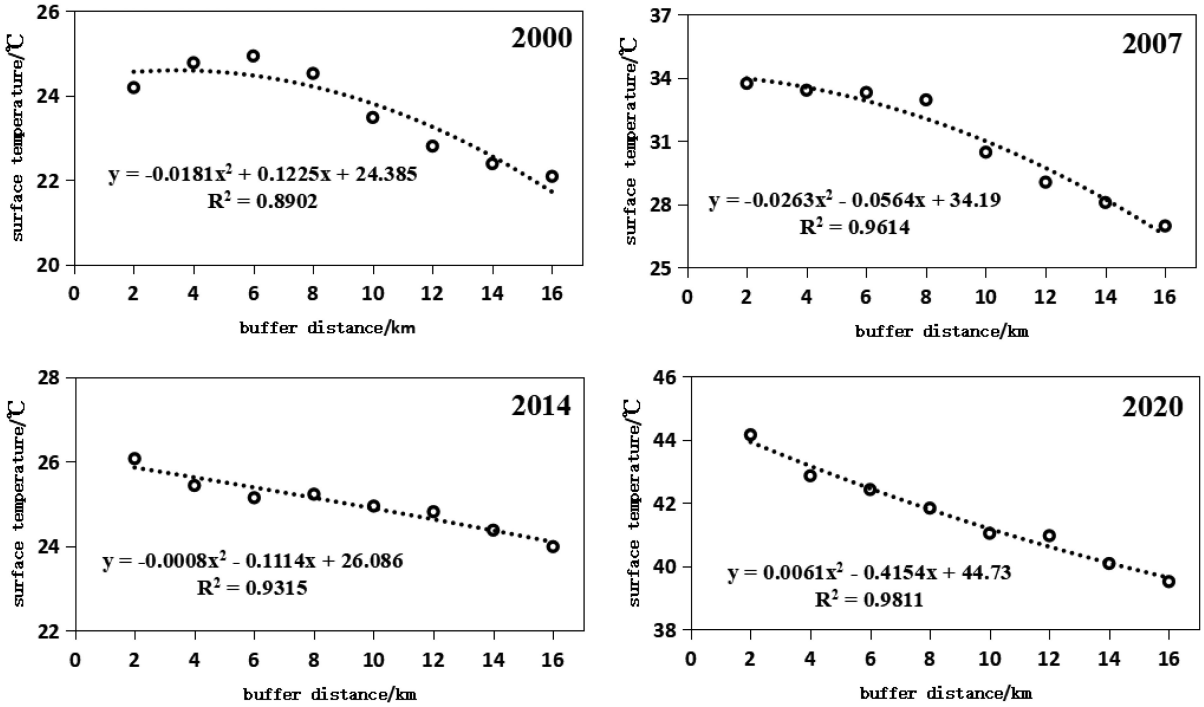

Fig. 8. Urban surface temperature gradient change function.

inner part of the city. This was because, at the end of the great development of urbanization, people have realized that many problems brought by the rapid development of urbanization, environmental awareness has been strengthened, urban green areas expanded, so that the area of highest temperature zone has been reduced. Polluting factories and enterprises were moving to the edge of the city, there would be the highest temperature zones on the edge of the city. The area of the higher temperature region increased obviously from 7.59% to 24.5%, and most of the changes came from the transformation of the highest temperature region. The area of the medium temperate zone decreased by 11.67%, and its distribution was less extensive.

In recent six years, the urbanization process has continued to enlarge and expanded to the north, but the highest temperature area was still mainly concentrated in the center of the city. The surface temperature of factories and enterprises in the southwest has changed from the highest temperature area to the higher temperature area and the medium temperature area. The area of the highest temperature area and the higher temperature area in the city was basically stable, and the area of the medium temperature area increased from 32.87% to 37.2%. It can be seen that the implementation and construction of urban greening have achieved initial results. The area of the lowest temperature area in the southeast has increased due to the impact of lakes, woodlands, and grasslands. The effect of patches of the natural vegetation on the cold and wet effect of the surface was obvious. The relevant government departments should pay attention to the large-area natural landscape planning of the urban boundary in the future.

E. Gradient Variation Characteristics of Heat Island Effect

Fig. 8 was the change in surface temperature from the center of Changchun to the suburbs and showed the overall trend of the declining gradient. Four years of urban surface gradient changes conformed to the law of quadratic polynomial function, R^2 was higher than 0.9, which clearly reflected the decrease in temperature during the transition from urban areas to suburbs.

It can be seen from the figure that the surface temperature rose slightly 2–6 km away from the city center in 2000, the temperature dropped significantly outside the 6 km buffer zone; in 2007, the surface temperature in the 0–8 km buffer zone at

TABLE IV
STATISTICAL TABLE OF LAND CLASSIFICATION MAP

Time	woodland (%)	grassland (%)	water area (%)	building land (%)
2000	3.54	71.05	1.99	23.42
2007	4.16	56.45	4.96	34.43
2014	7.13	48.46	4.85	39.56
2020	7.73	45.18	4.89	42.20

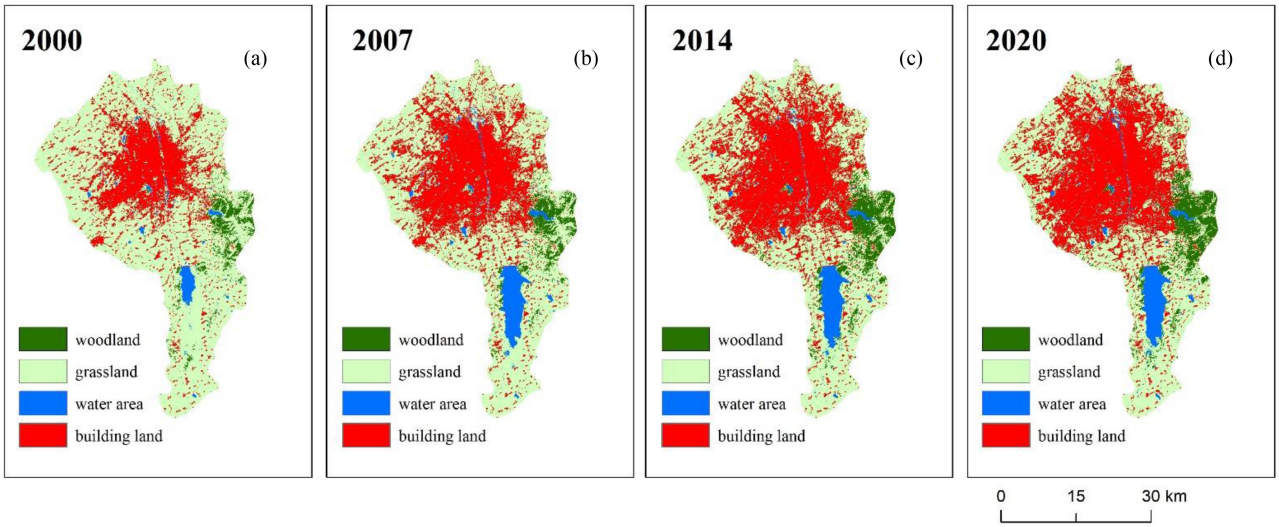

Fig. 9. Land type classification map of Changchun city.

a high level, while the temperature decreased after 8 km; the situation in 2014, the surface temperature showed an obvious decreasing trend from the urban center to the suburbs; the trend in 2020 was the same as that in 2014, but the range was greater.

The urban surface temperature increased first and then decreased with the increase of the buffer distance in 2000; the situation was different in 2007, 2014, and 2020, decreasing continuously with buffer distance. In the process of urbanization, its meteorological environment was affected, such as the enhanced greenhouse effect, and heat island effect significantly changed. From the perspective of gradient variation, in 2007, from the city center to the suburbs, the surface temperature changed the most. The UHI effect was strongest in this period; followed by 2020, the strength was not as strong as in 2014, but higher than in 2000 and 2007.

V. DISCUSSIONS

Urbanization was not only the general trend of development in all countries but also the symbol of national and human civilization and progress in the world [38]. As can be seen from Table IV and Fig. 9, in the past 20 years, the main land use structure of Changchun was mainly grassland, followed by building land. The proportion of water area and woodland was relatively small. With the realization of the occupation of human production and life to the natural environment, returning farmland to forest, grassland, and humidity has achieved initial results. However, the process of urbanization was still unstoppable.

It can be seen from Table IV that the proportion of grassland area has decreased significantly in 20 years, the area proportion decreased the most from 2000 to 2007, from 71.05% to 56.45%, the decrease rate of area proportion decreased from 2007 to 2020; the proportion of water area and woodland area increased slightly in 20 years, the area of water area increased from 1.99% to 4.89%, and the area of woodland increased from 3.54% to 7.73%; in 20 years, the proportion of building land has increased significantly, with the largest increase from 2000 to 2007, the increase rate decreased from 2007 to 2014, and urbanization slowed from 2014 to 2020. From the net change, the overall performance of grassland into building land.

Contrary to the trend of 2000–2014, the area of building land was still increasing, UHI effect decreased from 2014–2020. At the same time, the area of the highest temperature zone and higher temperature zone decreased during 2014–2020. First of all, the current urban expansion was mainly a pie-shaping style. Since 2014, the speed of urbanization has been slowed down and the boundaries of the suburbs have gradually blurred; second, the new urban area has a high rate of urban green space in response to the pursuit of ecological city construction policies [39]. Both of the above points have a significant mitigation effect on the UHI effect.

Combining the temperature distribution map and the land use type map, the corresponding temperature of different ground objects was calculated. As shown in Fig. 10, the results showed that different ground objected corresponding to different temperatures, and the average temperature of building land was

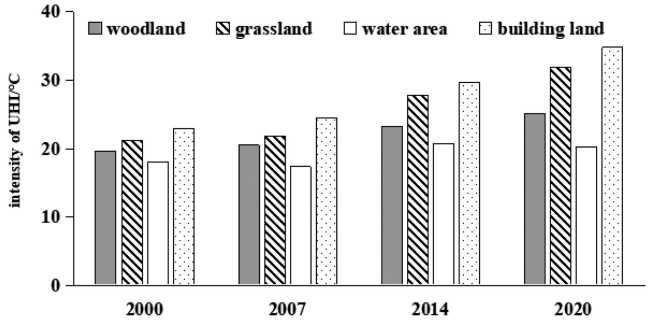

Fig. 10. Relationship between land type and urban surface temperature.

the highest, mainly distributed in high-temperature areas. The average temperature of grassland and woodland was relatively low and distributed in the low-temperature area, and the water area's average temperature was the lowest, distributed in the lowest temperature area.

The relationship between the average temperature of different ground objects was as follows: building land> grassland>woodland>water area. With the understanding that the construction land contributes the most to the UHI effect, scholars began to analyze the form of construction land in detail, and also pointed out that considering the factors such as area, height, and volume, the area has the most significant impact on the heat island effect [40]–[43]. This article only discussed the area of land type, the details such as the shape of buildings, the growth of vegetation, and the area and shape of water bodies whether there was a significant impact was not considered on the urban surface temperature. Some scholars even further explored ways to alleviate the heat island effect, so as to improve human living comfort [44].

The study of the heat island effect by remote sensing has the characteristics of large spatial scale and high precision, which would solve the problem of large spatial scale of the heat island effect. It was scientific to invert the temperature of ground objects by using the characteristics of thermal infrared radiation of ground objects, there were some errors due to the influence of atmosphere image and ground surface, but the result was relatively accurate.

VI. Conclusion

In this article, the temporal and spatial distribution characteristics of the UHI effect in Changchun City were studied. Including the temporal evolution characteristics of day, season, and year, as well as the spatial change characteristics of hierarchical and gradient. Then, combined with land use data, we analyzed the impact of the development of urbanization on the heat island effect.

Acknowledgment

The authors would like to thank all the organizations for sharing data.

References

[1] Z. Qiao and G. Tian, "Dynamic monitoring of footprint and capacity of Beijing heat Island based on Modis data from 2001 to 2012," *J. Remote Sens.*, vol. 19, no. 3, pp. 476–484, 2015.
[2] L. Howard, *The Climate of London: Deduced from Meteorological Observations, Made at Different Places in the Neighbourhood of the Metropolis*. vol. 1, London, U.K.: W. Phillips, 1818.
[3] S. W. Kim and R. D. Brown, "Urban heat island (UHI) intensity and magnitude estimations: A systematic literature review," *Sci. Total Environ.*, vol. 779, 2021, Art. no. 46389.
[4] M. Roth and W. T. Chow, "A historical review and assessment of urban heat island research in Singapore," *Singap. J. Trop. Geogr.*, vol. 33, no. 3, pp. 381–397, 2012.
[5] K. Zhang, R. Wang, C. Shen, and L. Da, "Temporal and spatial characteristics of the urban heat island during rapid urbanization in Shanghai, China," *Environ. Monit. Assess.*, vol. 169, no. 1, pp. 101–112, 2010.
[6] B. Y. Tam, W. A. Gough, and T. Mohsin, "The impact of urbanization and the urban heat island effect on day to day temperature variation," *Urban. Clim.*, vol. 12, pp. 1–10, 2015. doi: 10.1016/j.uclim.2014.12.004.
[7] S. Yang, X. Zhao, and S. Shen, "Study on seasonal characteristics of urban heat island in Beijing based on landsat TM /ETM + data," *J. Atmos. Sci.*, vol. 33, no. 4, pp. 427–435, 2010.
[8] H. Yoshikado and H. Kondo, "Inland penetration of the sea breeze over the Suburban area of Tokyo," *Bound Layer Meteor*, vol. 48, no. 4, pp. 389–407, 1989.
[9] H. Yoshikado, "Vertical structure of the sea breeze penetrating through a large urban complex," *Appl. Meteor.*, vol. 29, no. 9, pp. 878–891, 1990.
[10] H. Yoshikado and M. Tsuchida, "High levels of winter air pollution under the influence of the urban urban heat island along the shore of Tokyo Bay," *Appl. Meteor.*, vol. 35, no. 10, pp. 1804–1813, 1996.
[11] H. Kondo, "A numerical experiment on the interaction between sea breeze and valley wind to generate the so-called'Extended sea breeze," *Meteor. Soc. Jpn.*, vol. 68, pp. 435–446, 1990.
[12] H. Kondo, "The thermally induced local wind and surface inversion over the Kanto plain on calm winter nights," *Appl. Meteor.*, vol. 34, no. 6, pp. 1439–1448, 1995.
[13] F. Kimura and S. Takahashi, "The effects of land-use and anthropogenic heating on the surface temperature in the Tokyo metropolitan area: A numerical experiment," *Atmos. Environ.*, vol. 25, no. 2, pp. 155–164, 1991.
[14] Y. Ohashi and H. Kida, "Local circulations developed in the vicinity of both coastal and inland urban areas: A numerical study with a mesoscale atmospheric model," *Appl. Meteor.*, vol. 41, no. 1, pp. 30–45, 2002.
[15] Y. Ohashi and H. Kida, "Local circulations developed in the vicinity of both coastal and inland urban areas Part II: Effects of urban and mountain areas on moisture transport," *Appl. Meteor.*, vol. 43, no. 1, pp. 119–133, 2004.
[16] H. Kusaka, F. Kimura, H. Hirakuchi, and M. Mizutori, "The effects of land-use alteration on the sea breeze and daytime heat island in the Tokyo metropolitan area," *Meteor. Soc. Jpn.*, vol. 78, no. 4, pp. 405–420, 2000.
[17] H. P. Liu, J. C. L. Chan, and A. Y. S. Cheng, "Internal boundary layer structure under sea-breeze conditions in Hong Kong," *Atmos. Environ.*, vol. 35, no. 4, pp. 683–692, 2001.
[18] H. Tong, A. Walton, J. G. Sang, and J. C. L. Chan, "Numerical simulation of the urban boundary layer over the complex terrain of Hong Kong," *Atmos. Environ.*, vol. 39, no. 19, pp. 3549–3563, 2005.
[19] E. D. Freitas, C. M. Rozoff, W. R. Cotton, and P. L. S. Dias, "Interactions of an urban heat island and sea-breeze circulations during winter over the metropolitan area of So Paulo, Brazil," *Bound Layer Meteor.*, vol. 122, no. 1, pp. 43–65, 2007.
[20] J. Yang *et al.*, "Understanding land surface temperature impact factors based on local climate zones," *Sustain. Cities Soc.*, vol. 69, 2021, Art. no. 102818.
[21] A. Li, "Remote sensing analysis of Mianyang heat island effect based on RS," *Bull. Anhui Agronomy*, vol. 19, no. 13, pp. 143–148, 2013.
[22] D. Ma, "Analysis of urban heat island effect in Chaoyang," *J. Liaoning Teachers College*, vol. 10, no. 3, pp. 77–80, 2008.
[23] J. Yang *et al.*, "Optimizing local climate zones to mitigate urban heat island effect in human settlements," *J. Cleaner Prod.*, vol. 275, 2020, Art. no. 123767.
[24] Y. Wang, H. Du, Y. Xu, D. Lu, X. Wang, and Z. Guo, "Temporal and spatial variation relationship and influence factors on surface urban heat island and ozone pollution in the Yangtze River Delta, China," *Sci. Total Environ.*, vol. 631–632, pp. 921–933, 2018.

[25] Z. Chen, Y. Zhang, Y. Li, Z. Liu, X. Wang, and H. Meng, "Quantitative identification based on remote sensing technology in the northern city heat island effect change," *J. Jilin Univ.*, vol. 38, no. 3, pp. 325–334, 2020.
[26] C. Yang, F. Yan, and S. Zhang, "Comparison of land surface and air temperatures for quantifying summer and winter urban heat island in a snow climate city," *J. Environ. Manage.*, vol. 265, 2020, Art. no. 110563.
[27] Z. L. Li *et al.*, "Satellite-derived land surface temperature: Current status and perspectives," *Remote Sens. Environ.*, vol. 131, pp. 14–37, 2013.
[28] Z. H. Qin, A. Karnieli, and P. Berliner, "A mono-window algorithm for retrieving land surface temperature from landsat TM data and its application to the Israel-Egypt border region," *Int. J. Remote Sens.*, vol. 22, pp. 3719–3746, 2001.
[29] G. Tan, Z. Cai, and Y. Xu, "LANDSAT image-based heat island effect in Nanjing area," *Anhui Agric. Sci.*, vol. 37, no. 13, pp. 6050–6052, 2009.
[30] L. Wang, "Study on land surface temperature inversion and urban thermal environment in Xi'an based on RS," Chang'an Univ., Xi'an, China, 2015.
[31] B. Hai, "Study on the relationship between land surface temperature and rural industry development in rural areas," Henan Univ., Kaifeng, China, 2011.
[32] X. Wang, X. Li, and D. Xu, "Simulation analysis of microwave surface emissivity of vegetation cover based on CRTM," *Mod. Agric. Sci. Technol.*, vol. 24, pp. 220–221, 2017.
[33] Y. Liu, B. Yang, and C. Chen, "Spatio-temporal analysis of Urban heat island effect in Changsha based on remote sensing," *Remote Sens. Inf.*, vol. 6, pp. 73–78, 2011.
[34] H. Chang, "Vegetation coverage retrieval based on multi-source remote sensing," Qinghai Normal Univ., Xining, China, 2015.
[35] C. Sun, "Study and verification of multi-source remote sensing data fusion to generate high spatial-temporal resolution land surface temperature," Xi'an Univ. Sci. Technol., Xi'an, China, 2015.
[36] L. Li, "Spatio-temporal law and formation mechanism of changchun heat island effect," Northeast Normal Univ., Changchun, China, 2008.
[37] P. P. Li, "Land surface temperature retrieval and spatio-temporal pattern analysis in Nanjing based on environmental satellite data," Nanjing Agric. Univ., Nanjing, China, 2015.
[38] K. C. Seto, B. Guneralp, and L. R. Hutyra, "Global forecasts of urban expansion to 2030 and direct impacts on biodiversity and carbon pools," *Proc. Nat. Acad. Sci.*, vol. 109, no. 40, pp. 16083–16088, 2012.
[39] Y. Dong *et al.*, "Recording urban land dynamic and its effects during 2000–2019 at 15-m resolution by cloud computing with landsat series," *Remote Sens.*, vol. 12, no. 15, 2020, Art. no. 2451.
[40] Z. Qiao *et al.*, "Scale effects of the relationships between 3D building morphology and urban heat island: A case study of provincial capital cities of mainland China," *Complexity*, 2020, vol. 2020, Art. no. 9326793.
[41] J. Yang *et al.*, "Influence of urban morphological characteristics on thermal environment," *Sustain. Cities Soc.*, vol. 72, 2021, Art. no. 103045.
[42] J. Ren *et al.*, "Exploring thermal comfort of urban buildings based on local climate zones," *J. Cleaner Product.*, vol. 340, 2022, Art. no. 130744.
[43] C. Yang *et al.*, "Assessing the effects of 2D/3D urban morphology on the 3D urban thermal environment by using multi-source remote sensing data and UAV measurements: A case study of the snow-climate city of Changchun, China," *J. Cleaner Prod.*, vol. 321, 2021, Art. no. 128956.
[44] P. Xie *et al.*, "Urban scale ventilation analysis based on neighborhood normalized current model, sustainable cities and society," *Sustain. Cities Soc.*, vol. 80, 2022, Art. no. 103746.

Ziqi Chen received the B.S. degree in geography, in 2018, and the M.S. degree in cartography and geographic information systems, in 2021. She is currently working toward the Ph.D. degree in resources and environment from the College of Geo-Exploration Science and Technology, Jilin University, Changchun, China.

Her research interests include on ecological remote sensing assessment.

Yanhong Zhang received the Ph.D. degree from the Northeast Institute of Geography and Agroecology, Chinese Academy of Sciences, Changchun, China, in 2004.

She is currently an Associate Professor with the College of Geo-exploration Science & Technology, Jilin University, Changchun, China. Her research interests include application research of remote sensing and geographic information systems in resources and environment.